УДК 629.735
DOI: 10.26467/2079-0619-2026-29-2-106-120

Numerical study of helicopter airframe aerodynamics combined with coaxial main rotor using the URANS method

S.G. Konstantinov[1], P.V. Makeev[1], A.I. Shomov[1]
[1]Moscow Aviation Institute (National Research University), Moscow, Russia

Abstract: The work is dedicated to numerical modeling of Kamov Ka-226 helicopter aerodynamics for isolated helicopter airframe and helicopter airframe with coaxial main rotor. The CFD (computational fluid dynamics) method based on the URANS approach (Unsteady Reynolds-averaged Navier-Stokes equations) based on the Ansys Fluent software has been used. The hybrid overset mesh contained from 45 (isolated airframe) to 58 (airframe/rotor combination) million cells. The isolated helicopter airframe aerodynamic characteristics have been investigated for various airframe configurations such as: isolated fuselage, fuselage + tail, fuselage + tail + rotor head and fuselage + tail + rotor hub + landing gear (full configuration). The range of pitch angles from −16 to +16° has been considered. The full airframe/rotor combination aerodynamics has been investigated for a flight speed of 30 m/s. Comparison of calculated aerodynamic characteristics of isolated fuselage and full airframe configuration with wind tunnel (WT) test data has showed a satisfactory match. The results of numerical modelling of helicopter airframe aerodynamics have demonstrated specific features, such as: presence of negative lift force on the helicopters fuselage in horizontal flight and formation of two powerful vortex bundles behind the fuselage that affecting the tail stabilizer. The results of numerical modelling of helicopter airframe/rotor combination have allowed evaluating the effect of main rotor wake on the helicopter airframe aerodynamics. The performed study demonstrates the wide possibilities of the URANS approach in solving the complex problems of optimizing helicopter aerodynamics, taking into account the interference of airframe, its individual parts and main rotor.

Keywords: CFD, URANS method, helicopter airframe, coaxial main rotor, aerodynamic characteristics, aerodynamic interference.

For citation: Konstantinov, S.G., Makeev, P.V., Shomov, A.I. (2026). Numerical study of helicopter airframe aerodynamics combined with coaxial main rotor using the URANS method. Civil Aviation High Technologies, vol. 29, no. 2, pp. 106–120. DOI: 10.26467/2079-0619-2026-29-2-106-120

Численное исследование аэродинамики комбинации планера и соосного несущего винта вертолета на основе метода URANS

С.Г. Константинов[1], П.В. Макеев[1], А.И. Шомов[1]
[1]Московский авиационный институт (национальный исследовательский университет), г. Москва, Россия

Аннотация: Работа посвящена численному моделированию аэродинамических характеристик планера вертолета Камов Ка-226, а также комбинации планера и соосного несущего винта. Использован метод CFD (computational fluid dynamics) на основе подхода URANS (Unsteady Reynolds-averaged Navier-Stokes equations) с моделью турбулентности k-ω SST на базе пакета Ansys Fluent. Созданная для решения поставленных задач гибридная оверсетная расчетная сетка содержала от 45 миллионов (планер) до 58 миллионов (комбинация планера и несущего винта) ячеек. Характеристики планера вертолета рассчитаны для различных конфигураций, таких как изолированный фюзеляж, фюзеляж + оперение, фюзеляж + оперение + колонка автомата перекоса, фюзеляж + оперение + колонка автомата перекоса + шасси (полная конфигурация) в диапазоне углов атаки планера от −16 до +16°. Комбинация планера и несущего винта рассчитана в полной конфигурации для скорости полета 30 м/с. Сравнение расчетных аэродинамических характеристик изолированного фюзеляжа и планера вертолета в полной конфигурации с экспериментальными данными продувок в аэродинамической трубе показало удовлетворительное совпадение. Результаты численного моделирования аэродинамических характеристик планера продемонстрировали ряд особенностей: возникновение отрицательной подъемной силы на фюзеляже на режиме

горизонтального полета и формирование за ним двух мощных вихревых жгутов, оказывающих влияние на хвостовое оперение. Результаты численного моделирования аэродинамических характеристик комбинации планера и НВ позволили оценить также влияние вихревого следа НВ на аэродинамические характеристики планера. Выполненное исследование демонстрирует широкие возможности примененного подхода URANS для решения задач оптимизации аэродинамики вертолета с учетом интерференции его планера, отдельных частей и соосного несущего винта.

Ключевые слова: метод URANS, планер вертолета, соосный несущий винт, аэродинамические характеристики.

Для цитирования: Константинов С.Г., Макеев П.В., Шомов А.И. Численное исследование аэродинамики комбинации планера и соосного несущего винта вертолета на основе метода URANS // Научный вестник МГТУ ГА. 2026. Т. 29, № 2. С. 106–120. DOI: 10.26467/2079-0619-2026-29-2-106-120

Introduction

The aerodynamics of the helicopter airframe significantly affects its flight performance. Therefore, the choice of the optimal configuration of the airframe, taking into account the interference between its individual elements, as well as the main rotor, is an important task.

Solving such problems requires complex and expensive experimental studies, especially if it is necessary to model the aerodynamic characteristics of the helicopter airframe with main rotor. In this regard, the possibility of numerical modeling of the aerodynamic characteristics of an isolated helicopter airframe, as well as a helicopter airframe, taking into account the induced effects of main rotor, is of interest. Potentially, such an approach can significantly complement the results of experimental studies and reduce their costs. The current level of supercomputer technologies and numerical modeling methods has led to the possibility of practical implementation of such tasks. As a result, in the last two decades, a number of research papers has been published on the aerodynamic characteristics of helicopter fuselages (airframes) including the main and tail rotors influence, based on various numerical methods.

Thus, in paper [1] three different CFD packages are used: OVERFLOW 2.0, elsA and FUN3D. In all three cases, the RANS (Reynolds-averaged Navier-Stokes equations) approach is used. The aerodynamic characteristics of the Dauphin helicopter (fuselage + tail) in an isolated formulation are considered, as well as taking into account the influence of the main rotor (active disk model). In the work by [2], on the basis of the original CFD package HMB (Helicopter Multi-Block), a specialized test task ROBIN (Rotor Body Interaction) from NASA (isolated fuselage with main rotor) and a task within the GOAHEAD project (Generation of Advanced Helicopter Experimental Aerodynamic Database for CFD code validation) are solved. In [3] an original approach based on the VTM (Vorticity Transport Method) method has been used to solve the ROBIN test. In [4] on the basis of the CFD solver proposed by the authors, together with the ROBIN test, the complete configuration of the UH-60 helicopter airframe, including the main and tail rotors have been considered. In [5] have used the FUN3D CFD package (URANS approach) and the CHARM CFD package (vortex method) to study the interaction of the fuselage and rotor. In the article by [6], an EC-135 helicopter (fuselage + rotor head + tail + main and tail rotors) has been modeled on the basis of the FLOWer CFD package (URANS approach). The work focuses on the study of the influence of the main rotor hub fairing on the aerodynamics of the helicopter. In [7], an original vortex method is used to solve test problems for a combination of fuselage and rotor. In the article by [8] based on the CFD package Star-CCM+ (URANS approach), the aerodynamic characteristics of an isolated fuselage have been investigated. In the work by [9], the CFD package FLUENT has been used to analyze the interference of the fuselage and the main rotor, also using the URANS approach. In the article by [10], the interference of the rotor and the fuselage of a helicopter has been investigated on the basis of an original unsteady panel/vortex model. In [11], CFD/CSD (computational structural dynamics) studies have been performed for the Sikorsky X-2 ABC (Advanced Blade Concept)

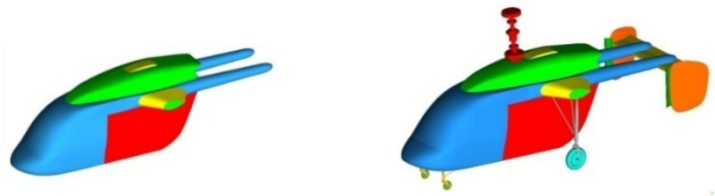

a b

Fig. 1. Models of isolated fuselage (a) and full airframe (b)

technology demonstrator helicopter (fuselage + tail + coaxial rotor). The PRASADUM CSD package and the CREATE-AV CFD package, which includes the OVERFLOW CFD package (URANS approach), have been used. In [12] the effect of the main rotor on the tail boom of a helicopter based on the CFD package HMB (Helicopter Multi-Block) using the URANS approach was investigated. The work by [13] uses the original CFD package to simulate the test of main rotor and fuselage (cylinder body) interference from GIT (Georgia Institute of Technology). In [14], two CFD packages are used to model the aerodynamics of an isolated fuselage: PUMA and FLUENT. [15] in their article also use two different CFD packages with the URANS approach: STAR-CCM+ and CREATETM-AV. The aerodynamics of the fuselage and rotor combination and their interaction with the tail are simulated. In [16] based on the CFD approach, the aeroacoustics problem for a combination of a coaxial rotor and a fuselage is considered. One of the newest works in the field under consideration is the article [17], which examines the interference of the body and propellers of an unmanned quadcopter. Another work by [18, 19] is devoted to the study of interference between the main and tail rotors of a single-rotor helicopter (taking into account the fuselage). Both of these works also use the URANS approach.

Thus, nowadays modern CFD methods of numerical modeling are widely used to solve various problems related to the aerodynamics of the helicopter fuselage/rotors combinations. The URANS approach, which combines relatively moderate requirements for computing resources, vast opportunities for aerodynamic analysis, and sufficient accuracy of the results obtained, has now become the most widespread. At the same time, most of the works published on this topic consider an isolated fuselage and focus on the validation of various CFD codes. Works considering the combination of helicopter rotors and full airframe, including the fuselage, tail, rotor hub, landing gear and other elements are still quite rare.

In the presented work, two tasks are solved on the basis of the Ansys Fluent CFD package and the URANS approach. The first is the study of the aerodynamic characteristics of the isolated airframe of the Ka-226 helicopter (in various configurations) in a wide range of angles of attack. The second is modeling the aerodynamics of a combination of helicopter airframe and coaxial main rotor in forward flight.

Research methods and methodology

The calculation of the aerodynamic characteristics of the Ka-226 helicopter airframe (fig. 1) [20] has been carried out for pitch angles α from −16 to +16° with an interval $\Delta\alpha = 4°$ for two Reynolds numbers. The Reynolds number $Re = 7.2 \cdot 10^6$ corresponds to the conditions of the experiment conducted for the model of Ka-226 airframe in WT and is described in paper [19]. The Reynolds number $Re = 1.7 \cdot 10^7$ is a full-scale and corresponds to the forward flight mode of a helicopter with a speed of V = 30 m/s. The Reynolds number was calculated for the length of the fuselage LF = 6.62 m.

For calculations, a hybrid mesh has been created, consisting of separate zones united by an overset interface, containing about 45 million cells (fig. 2). The calculation area has had a cy-

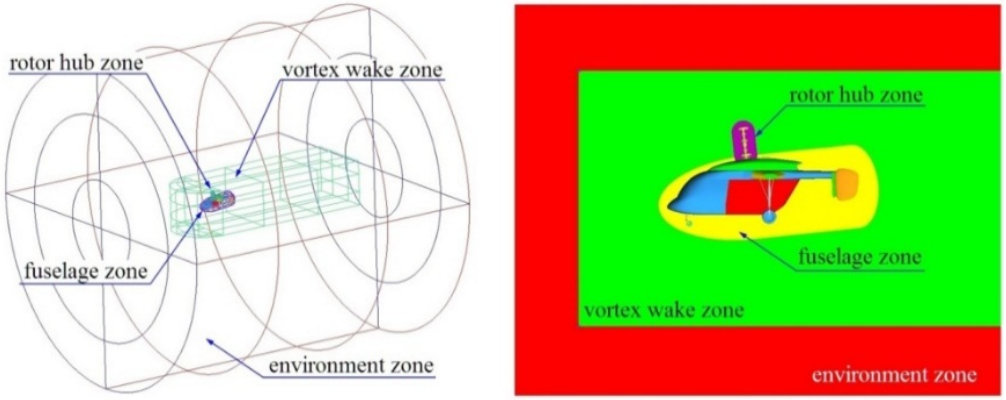

Fig. 2. Computational volume zones scheme

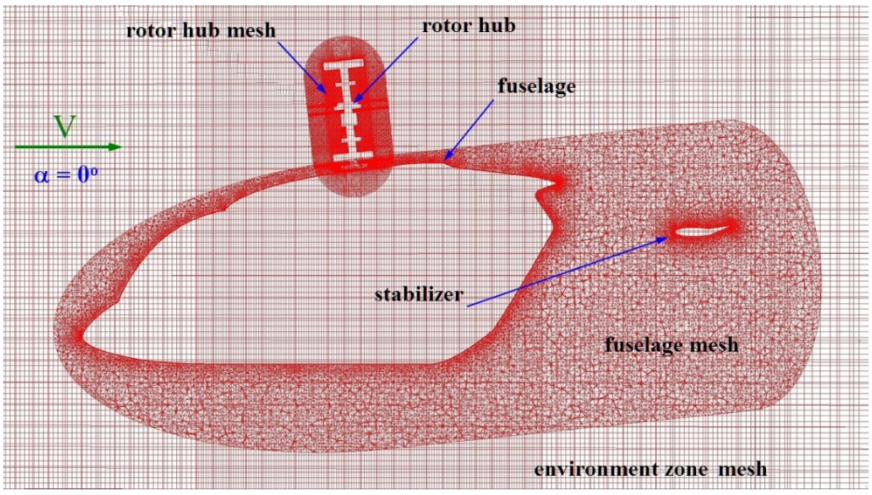

Fig. 3. The structure of computational mesh in the plane of symmetry of the helicopter

lindrical shape. The boundaries of the design area have been located at a distance of $15L_F$ (here L_F is the length of the fuselage) on the side and in front of the helicopter airframe, with the exception of the output boundary, which has been distant by $25L_F$. The surface mesh of the airframe and its elements was constructed in such a way that the first mesh node has been located in the region of the viscous velocity profile $Y + \leq 1$ (fig. 3). Preliminary studies of mesh convergence have shown that the quality of the calculated mesh and the mesh resolution are sufficient to solve the task.

Numerical modelling has been carried out in an unsteady formulation and covered changes in the flow parameters over time. In the calculations there has been used the finite volume method based on the URANS approach (Unsteady Reynolds-Averaged Navier-Strokes Equations) with a k-ω SST turbulence model. The parameters of the initial turbulence have been selected based on the conditions of the average intensity of the developed turbulent flow. The value of the relative turbulent viscosity has been assumed to be 5. The value of the turbulent intensity has been assumed to be 1%.

The aerodynamic characteristics of the airframe, taking into account the effect of the induced flow from the coaxial main rotor of the Ka-226 helicopter, have been calculated for the forward flight speed V = 30 m/s ($Re = 1.7 \cdot 10^7$) and pitch angle $\alpha = 1.3°$. The coaxial main rotor

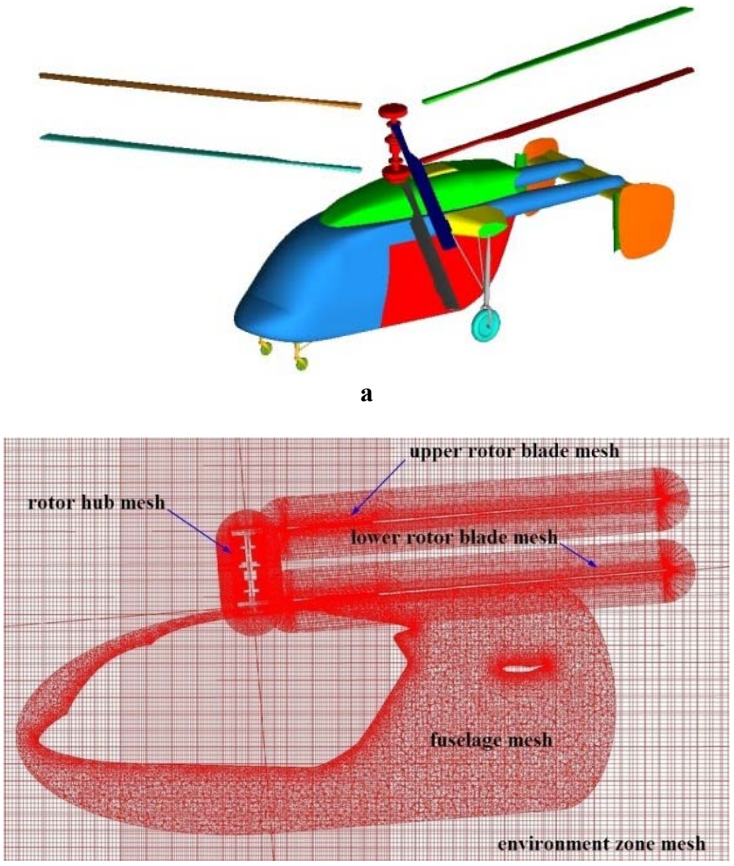

a

b

Fig. 4. Model of airframe/rotor combination (a) and structure of the computational mesh in the plane of symmetry (b)

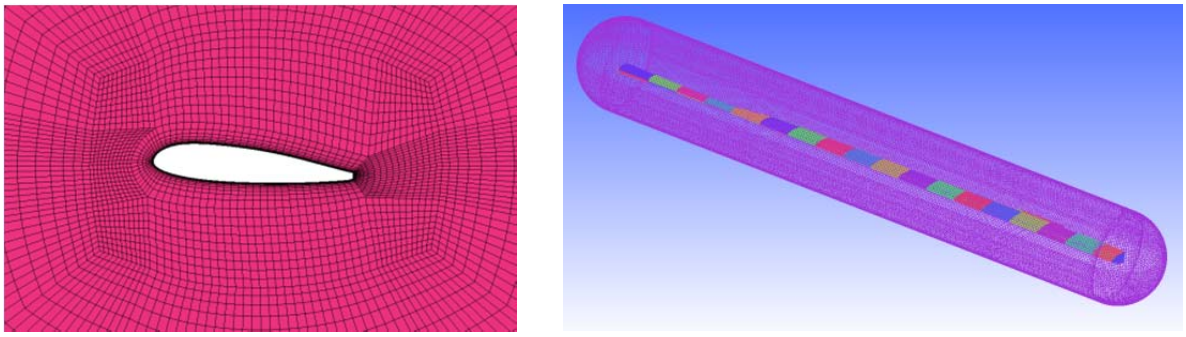

a b

Fig. 5. The structures of the mesh in the cross section (a) and the surface mesh (b) of the rotor blade

has had the following parameters: radius of the rotor R = 6.62 m; rotor solidity σ = 0.075; rotor blade tip speed ωR =198.3 m/s; blade twist θΣ = −8.35°; blade chord c = 0.26 m; number of blades $N_b = 2 \times 3$.

For the calculations, the basic helicopter airframe mesh has been used. The zones of the rotor blades have been added to this mesh. Total meshes have been combined using an overset interface (fig. 4 and fig. 5). The final calculated mesh eventually contained about 58 million cells and has been constructed at the surface of the blades in such a way that the first node of the mesh has been in the region of the viscous velocity profile $Y + \leq 1$. Preliminary studies of mesh convergence have shown that the quality of the calculated mesh and the mesh resolution are sufficient to solve the task.

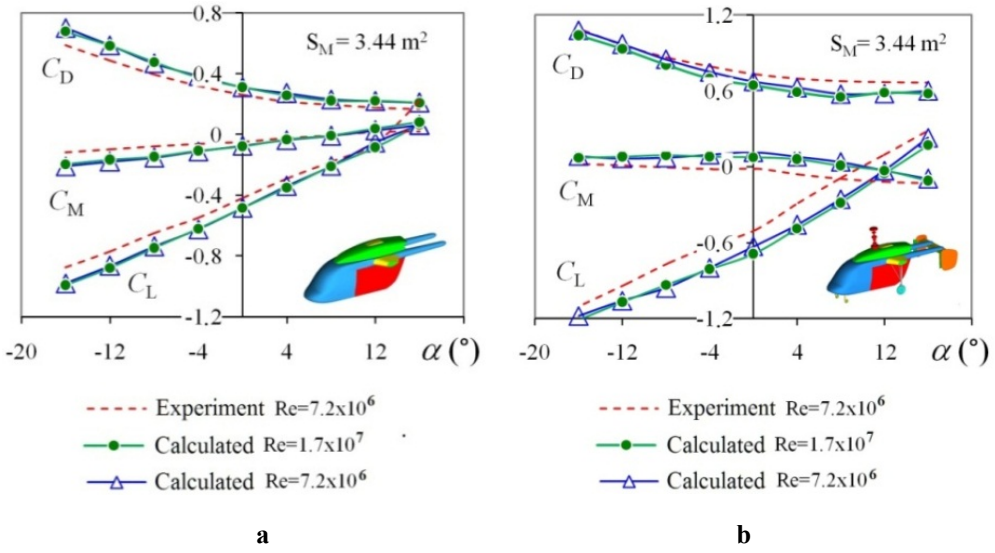

a **b**

Fig. 6. Calculated and experimental dependencies of the drag C_D, lift C_L and pitch moment C_M coefficients for isolated fuselage (a) and full airframe (b)

The numerical modelling for helicopter airframe/rotor combination has been carried out in the same formulation and with the same environmental conditions and properties as for the isolated helicopter airframe studying.

Upper and lower rotor collective and cyclic pitch laws have been corresponded to the flight of Ka-226 helicopter with forward flight speed V = 30 m/s. These rotor control laws have been determined in preliminary studies using the free wake model developed at MAI. The free wake model is described in the work [21] dedicated to numerical simulation of an isolated Ka-226 coaxial main rotor aerodynamics. The upper and lower rotors have been balanced in torque. The rotor blades have been modeled to be absolutely rigid for bending and twisting.

Results and Discussion

Figure 6 shows calculated dependencies of the lift force C_L, drag force C_D and pitching moment C_M coefficients on the angle of attack α and on the Reynolds number Re for isolated fuselage (fig. 6, *a*) and full airframe (fig. 6, *b*) of the helicopter. Aerodynamic coefficients are relative to the area of fuselage cross-section SM = 3.44 m^2. Comparison of calculated and experimental [19] data showed satisfactory coincidence. Analysis of calculated results of helicopter airframe with landing gear and main rotor hub in comparison with an isolated helicopter fuselage showed the influence of the local Re number on the aerodynamic characteristics of the helicopter airframe elements. This effect is important to take into account when conducting experimental studies. Also, the diagrams in the Figure 6 show that helicopter airframe has a negative lifting force in forward flight, that requires an additional power to compensate it.

Figure 7 shows calculated dependencies between the lift force C_L, drag force C_D and pitching moment C_M coefficients and the angle of attack α for different airframe configurations. Coefficients pitching moment CM was calculated for the center of weights of the helicopter. Separately, data are given for 4 configurations: isolated fuselage, fuselage + tail, fuselage + tail + rotor hub, fuselage + tail + rotor hub + landing gear. These graphs allow estimating the contribution of various elements of the airframe to the resulting full aerodynamic characteristics.

An important advantage of modern numerical methods is the ability to determine not only total, but also distributed aerodynamic characteristics, such as pressure distribution over the surface. In addition, they make it possible to analyze in detail the flow and the wake structure behind the object.

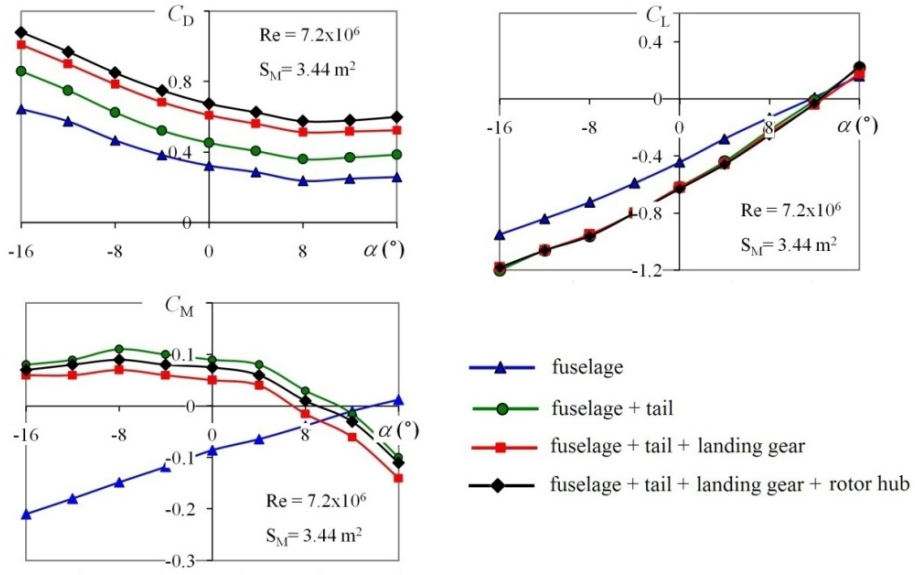

Fig. 7. Calculated dependencies of the drag C_D, lift C_L and pitch moment C_M coefficients for isolated fuselage and various airframe configurations

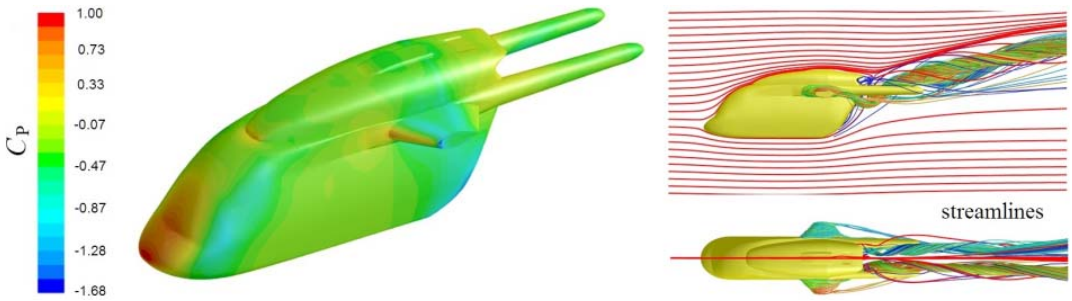

Fig. 8. Distribution of the pressure coefficient (a) over the surface and visualization of the flow around isolated helicopter fuselage using streamlines (b)

Figure 8 shows the distribution of the pressure coefficient c_p over the surface of isolated helicopter fuselage and flow visualization. It can be seen, that the airframe flow is accompanied by the formation of two vortex bundles falling from the back of fuselage into the area of the helicopter's tail. These vortices will have a significant induced effect on the vertical and horizontal stabilizers. Therefore, at the stage of developing the layout of the helicopter, the tail must be positioned taking into account the flow structure around the helicopter. To improve the airframe aerodynamics in this case the different shapes of the back of fuselage may be considered.

An important advantage of modern numerical methods is the ability to determine not only total, but also distributed aerodynamic characteristics, such as pressure distribution over the surface. In addition, they make it possible to analyze in detail the flow and the wake structure behind the object.

Figure 9 shows the velocity V (fig. 9, *a*) and vorticity ω (fig. 9, *b*) fields in the longitudinal section of computational mesh for isolated fuselage. Figure 10 shows the velocity (fig. 10, *a*) and vorticity (fig. 10, *b*) fields for full helicopters airframe with tail, landing gear and rotor hub. Pitch angles of −8 and 4 degrees are presented in Figures 9 and 10. These results give a

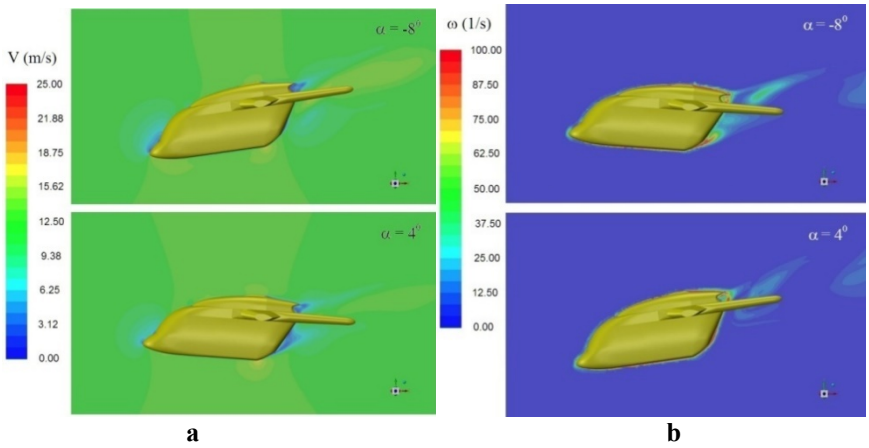

Fig. 9. Velocity fields (a) and vorticity contours (b) of isolated fuselage: Re = $7.2 \cdot 10^6$

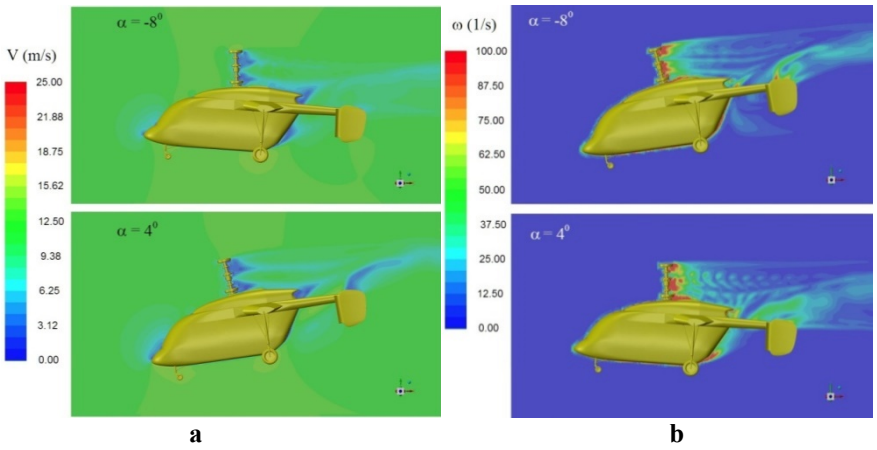

Fig. 10. Velocity fields (a) and vorticity contours (b) of full airframe: Re = $7.2 \cdot 10^6$

qualitative representation of the flow around the helicopters airframe. It can be seen that the tail is in a disturbed flow formed due to the flow around the rotor hub and back of fuselage (fig. 10). Also, there are clearly visible areas of full flow braking and areas of flow disturbance leading to an increase in the overall helicopters drag (fig. 9 and fig.10).

Figure 11 shows the field of total velocity V and vorticity ω in the longitudinal section of the computational domain. The figures clearly show the vorticity regions corresponding to the locations of the tip and root vortex filaments, which, downstream of the rotor, are smeared due to diffusion, forming a continuous vorticity region**.**

Figure 12 shows the flow patterns around the helicopter airframe and the combination of the helicopter airframe with the main rotor in the longitudinal section of the computational domain. It can be seen that the flow pattern around the tail empennage, which is located in the induced flow of the main rotor, differs significantly from the flow pattern around the airframe without the main rotor.

Figure 12 shows that the influence of the main rotor is reflected in the aerodynamic characteristics of the airframe. Specifically, the influence of the main rotor slightly reduces the drag of the airframe and increases the negative lift on the fuselage.

Figure 13 shows visualization of the structure of the helicopter vortex wake using isosurfaces (for $\omega = 25\ s^{-1}$). The presented pictures demonstrate the well-known features of the main rotor

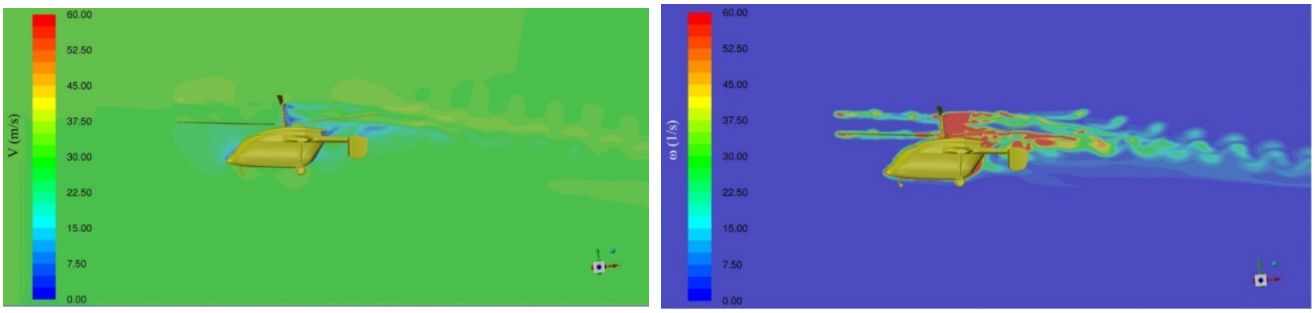

a **b**

Fig. 11. Velocity fields (a) and vorticity contours (b) of airframe/rotor combination at forward flight: V = 30 m/s; α = 1.3°; Re = 7,2 · 10^6

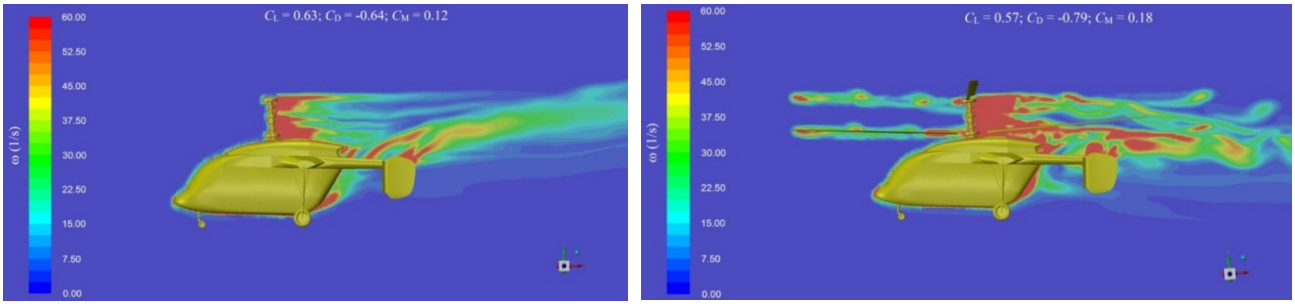

a **b**

Fig. 12. Vorticity contours of isolated airframe (a) and airframe/rotor combination (b) at forward flight: V = 30 m/s; α = 1.3°; Re = 7.2 · 10^6

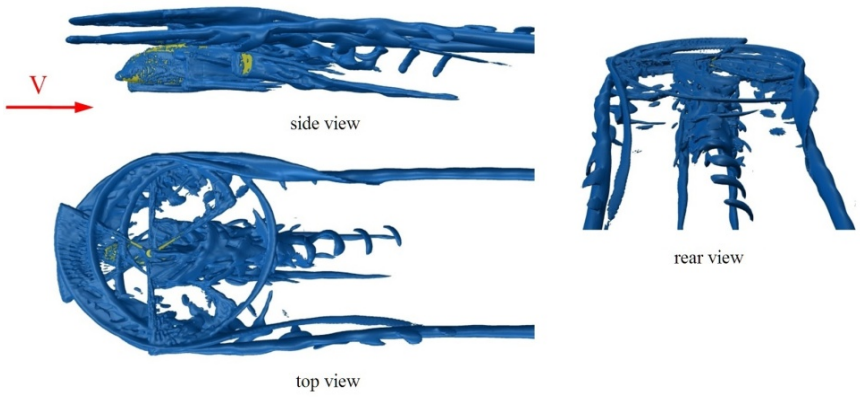

Fig. 13. Visualization of the structure of the vortex wake using isosurfaces (ω = 25 s^{-1})

vortex wake at forward flight [22]. Blade-vortex interactions and structures of the right and left super vortices formed behind the main rotor are clearly visible here. There is also a visible wake behind the fuselage and the tail. Also, Figure 13 clearly shows the regions of interaction between the blades and the tip and root vortices.

Figure 14 shows the diagrams of the vertical component of induced velocity V_y (fig. 14, *a*) plotted along the lines lying in the plane of rotation of the lower rotor at a distance of X/R = −0.5; −1.0 and −1.5 (fig. 14, *b*). Here is a pattern characteristic of the main rotor wake in forward flight mode. There is a downward in-

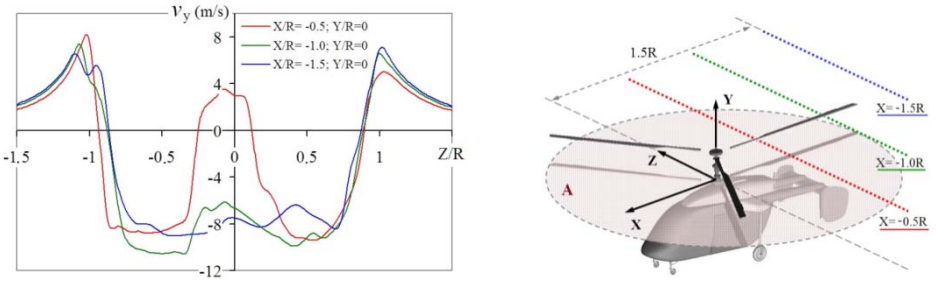

a **b**

Fig. 14. Plots (a) of the vertical component of the induced velocity V_y calculated along the lines (b) lying in the plane of rotation (plane "A") of the lower rotor

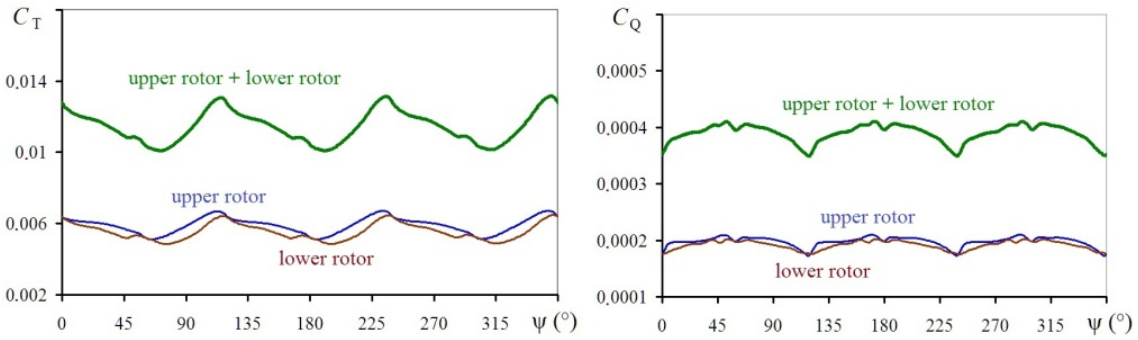

a **b**

Fig. 15. The dependencies of the thrust (a) and torque (b) coefficients of the coaxial main rotor for one revolution at the forward flight (V = 30 m/s)

duced flow between the right and left super vortices (fig. 13). At the right and left edges, the induced flow is directed upwards.

Figure 15 shows the dependencies of the coaxial main rotor thrust coefficients CT (fig. 15, *a*) and the torque coefficients CQ (fig. 15, *b*) constructed for one revolution of the rotor. The coefficients for the lower and upper rotors and their sum are given separately. It can be seen that the thrust and torque of the coaxial main rotor pulsate over time, due to the aerodynamic interference of the upper and lower screws. This feature of coaxial rotor is noted in a number of works [21, 23, 24]. From the Figure 15, *b* it also follows that the torque of the lower and upper rotors is balanced.

Conclusion

Numerical simulation of aerodynamic characteristics of Kamov Ka-226 helicopter for various configurations at forward flight with speed of V = 30 m/s has been performed. An isolated helicopter airframe in the range of pitch angles −16...+16 degrees and combination of airframe with coaxial main rotor for pitch angle 1.3 degree have been considered.

The URANS method with the k-ω SST turbulence model based on the Ansys Fluent software package has been used. The developed unstructured overset computational mesh which contained from 45 to 58 million cells and has provided high quality of the results obtained.

Comparison of the calculated helicopter airframe aerodynamic characteristics with experimental data has shown a good qualitative and quantitative coincidence. That confirms the reli-

ability and sufficient accuracy of the applied calculation method and mesh.

As a result of numerical modelling, the influence of the local Reynolds number on the aerodynamic characteristics of such elements of the helicopter airframe as landing gear and main rotor hub has been identified. It is shown that in the forward flight mode, powerful vortex bundles are formed behind the fuselage affecting the helicopter tail, which has to be taken into consideration while choosing the tail unit parameters. It is also established that the helicopter airframe has a negative lifting force in forward flight modes, which requires additional power costs. One of the ways to overcome this effect is to optimize the shape of the fuselage back.

For the airframe/rotor combination a modelling of the forward flight, taking into account helicopter balancing, has been carried out. Flow patterns and aerodynamic characteristics have been calculated and analyzed. The main features associated with the operation of the main rotor in forward flight have been demonstrated. Formation of the left and right super vortices behind the rotor has been shown. Pulsations of thrust and torque coefficients due to interference between the upper and lower rotors have been obtained. The influence of the main rotor on the helicopter airframe has been analyzed. It has been found the decrease of airframe drag in 10%, increase of negative lift force on the airframe in 23% and increase of pitch moment in 50 %.

The results presented in this paper can make a significant contribution to the experience of using numerical modeling methods in solving the problem of calculating the aerodynamic characteristics of a full helicopter airframe with coaxial main rotor.

References

1. Renaud, T., O'Brien, D., Smith, M., Potsdam, M. (2008). Evaluation of isolated fuselage and rotor-fuselage interaction using CFD. *Journal of the American Helicopter Society*, vol. 53, no. 1, pp. 3–17. DOI: 10.4050/JAHS.53.3

2. Steijl, R., Barakos, G. (2008). Computational analysis of rotor-fuselage interactional aerodynamics using sliding-plane CFD method. *ResearchGate*, 16 p. Available at: https://www.researchgate.net/publication/266096529_Computational_analysis_of_rotor-fuselage_interactional_aerodynamics_using_sliding-plane_CFD_method (accessed: 17.06.2025).

3. Smith, M., Shenoy, R., Kenyon, A., Brown, R. (2009). Vorticity-transport and unstructured RANS investigation of rotor-fuselage interactions. *In: 35th European Rotorcraft Forum*, Hamburg, Germany, 19 p. Available at: https://dspace-erf.nlr.nl/server/api/core/bitstreams/783e9f1d-0503-44bd-acea-48b1636888e0/content (accessed: 17.06.2025).

4. Lee, B., Jung, M., Kwon, O.-J., Kang, H.J. (2010). Numerical simulation of rotor-fuselage aerodynamic interaction using an unstructured overset mesh technique. *International Journal of Aeronautical and Space Sciences*, vol. 11, issue 1, pp. 1–9. DOI: 10.5139/IJASS.2010.11.1.001

5. Quon, E., Smith, M., Whitehouse, G., Wachspress, D. (2012). Unsteady reynolds-averaged navier-stokes-based hybrid methodologies for rotor-fuselage interaction. *Journal of Aircraft*, vol. 49, no. 3, pp. 961–965. DOI: 10.2514/1.C031578

6. Schäferlein, U., Keßler, M. (2014). CFD-simulation of the rotor head influence to the rotor-fuselage interaction. *In: 40th European Rotorcraft Forum*, Southampton, United Kingdom, 12 p. Available at: https://dspace-erf.nlr.nl/server/api/core/bitstreams/0f0f46c2-f81a-47af-9a73-40c3d6589cf8/content (accessed: 17.06.2025).

7. Tan, J., Wang, H. (2014). Numerical analysis of helicopter rotor/fuselage unsteady aerodynamic interaction. *Acta Aerodynamica Sinica*, vol. 32, no. 3, pp. 320–327. DOI: 10.7638/kqdlxxb-2012.0141

8. Nicolosi, F., Vecchia, P., Ciliberti, D., Cusati, V. (2015). Fuselage aerodynamic drag prediction method by CFD. *In: 5th CEAS Air & Space Conference*, Delft, NL, 7–11 September. Available at: https://www.researchgate.net/publication/332407449_Fuselage_aerodynamic_drag_prediction_method_by_CFD (accessed: 17.06.2025).

9. Açıkgöz, M.B., Aslan, A.R. (2016). Dynamic mesh analyses of helicopter rotor–fuselage flow interaction in forward flight. *Journal of Aerospace Engineering*, vol. 29, no. 6, ID: 04016050. DOI: 10.1061/(ASCE)AS.1943-5525.0000641 (accessed: 17.06.2025).

10. Dawei, L., Ji, X., Jun, H. (2016). The theoretical research for the rotor/fuselage unsteady aerodynamic interaction problem. *Journal of Aerospace Technology and Management*, vol. 8, no. 3, pp. 281–288. DOI: 10.5028/jatm. v8i3.686

11. Passe, B., Sridharan, A., Baeder, J., Singh, R. (2016). Identification of rotor-fuselage aerodynamic interactions in a compound coaxial helicopter using CFD-CSD Coupling. *In: American Helicopter Society Specialists Meeting on Aeromechanics Design for Vertical Lift*, San Francisco, CA, 20–22 January. Available at: https://www.researchgate.net/publication/296467339_Identification_of_Rotor-Fuselage_Aerodynamic_nteractions_in_a_Compound_Coaxial_Helicopter_using_CFD-CSD_Coupling (accessed: 17.06.2025).

12. Batrakov, A., Kusyumov, A., Kusyumov, S., Mikhailov, S., Barakos, G. (2017). Simulation of tail boom vibrations using main rotor-fuselage computational fluid dynamics (CFD). *Applied Sciences*, vol. 7, issue 9, ID: 918. DOI: 10.3390/app7090918 (accessed: 17.06.2025).

13. Xu, H., Xing, S.-L., Ye, Z.-Y., Ma, M.-S. (2016). A simple and conservative unstructured sliding-mesh approach for rotor-fuselage aerodynamic interaction simulation. *Proceedings of the Institution of Mechanical Engineers, Part G: Journal of Aerospace Engineering*, vol. 231, issue 1, pp. 163–179. DOI: 10.1177/0954410016664919

14. Aiman, W.A., Mohd, N.A.R.N., Mat, S., Dahalan, N.B. (2018). Numerical modelling of helicopter fuselage aerodynamics in forward flight using computational fluid dynamics. *In: 3rd South East Asia Workshop on Aerospace Engineering*, Bangkok, Thailand, 6-8 September. Available at: https://www.researchgate.net/publication/332038050_NUMERICAL_MODELLING_OF_HELICOPTER_FUSELAGE_AERODYNAMICS_IN_FORWARD_FLIGHT_USING_COMPUTATIONAL_FLUID_DYNAMICS (accessed: 17.06.2025).

15. Lorber, P., Min, B.-Y., Zhao, J. (2019). Comparison of rotor - fuselage flow fields and unsteady tail interactions between two CFD codes and experiment. *In: 75th Annual Forum of the American Helicopter Society*, Philadelphia, Pennsylvania, USA, 13–16 May. DOI: 10.4050/F-0075-2019-14500 (accessed: 17.06.2025).

16. Kim, J., Ko, J., Lee, S. (2019). Aeroacoustic analysis of coaxial rotor with rotor-fuselage interaction. *In: 48 th International Congress and Exhibition on Noise Control Engineering*, Madrid, Spain, 16–19 June. Available at: https://www.sea-acustica.es/INTERNOISE_2019/Fchrs/Proceedings/1812.pdf (accessed: 17.06.2025).

17. Zhu, Y., Lin, D., Mo, L., Lv, P., Ye, J. (2021). Numerical study of the aerodynamic interference of rotors imposed on fuselage for a quadcopter. *IEEE Access*, vol. 9, pp. 150021–150036. DOI: 10.1109/ACCESS.2021.3124507 (accessed: 17.06.2025).

18. Wang, C., Huang, M., Ma, S., Wang, H., Tang, M. (2021). Main rotor wake interference effects on tail rotor thrust in crosswind. *International Journal of Aerospace Engineering*, vol. 2021, ID: 9994115, 13 p. DOI: 10.1155/2021/9994115 (accessed: 17.06.2025).

19. Anikin, V.A., Voyevodin, A.V., Kolomensky, D.S., Sudakov, G.G. (2005). Helicopter hull streamlining calculated with help of Reynolds equations. *Polet. Obshcherossiyskiy Nauchno-Tekhnicheskiy Zhurnal*, no. 11, pp. 43–48. (in Russian)

20. Ignatkin, Yu.M., Konstantinov, S.G. (2017). Researches of aerodynamic characteristics of planer helicopters using CFD-method. *All-Russian Scientific-Technical Journal "Polyot" ("Flight")*, no. 9-10, pp. 34–41. (in Russian)

21. Konstantinov, S.G., Ignatkin, Yu.M., Makeev, P.V., Nikitin, S.O. (2021). Comparative study of coaxial main rotor aerodynamics in the hover with the usage of two methods of computational fluid dynamics. *Journal of Aerospace Technology and Management*, vol. 13, 14 p. DOI: 10.1590/jatm.v13.1210 (accessed: 17.06.2025).

22. Ignatkin, Yu., Makeev, P., Konstantinov, S., Shomov, A. (2020). Modelling the helicopter rotor aerodynamics at forward flight with free wake model and URANS method. *Aviation*, vol. 24, no. 4, pp. 149–156. DOI: 10.3846/aviation. 2020. 12714

23. Kritsky, B.S., Mirgazov, R.M., Anikin, V.A., Gerasimov, O.V. (2020). Thrust pulsation of coaxial main rotor, caused by the blades relative position. *Civil Aviation High Technologies*, vol. 23, no. 4, pp. 96–104. DOI: 10.26467/2079-0619-2020-23-4-96-104

24. Kim, H., Brown, R. (2010). A comparison of coaxial and conventional rotor performance. *Journal of the American Helicopter Society*, vol. 55, no. 1, pp. 12004. DOI: 10.4050/JAHS.55.012004

Список литературы

1. Renaud T. Evaluation of isolated fuselage and rotor-fuselage interaction using CFD / T. Renaud, D. O'Brien, M. Smith, M. Potsdam // Journal of the American Helicopter Society. 2008. Vol. 53, no. 1. Pp. 3–17. DOI: 10.4050/JAHS.53.3

2. Steijl R., Barakos G. Computational analysis of rotor-fuselage interactional aerodynamics using sliding-plane CFD method [Электронный ресурс] // ResearchGate. 2008. 16 p. URL: https://www.researchgate.net/publication/266096529_Computational_analysis_of_ rotor-fuselage_interactional_aerodynamics_using_ sliding-plane_CFD_method (дата обращения: 17.06.2025).

3. Smith M. Vorticity-transport and unstructured RANS investigation of rotor-fuselage interactions / M. Smith, R. Shenoy, A. Kenyon, R. Brown [Электронный ресурс] // 35th European Rotorcraft Forum. Germany, Hamburg, 2009. ID: 101271. 19 p. URL: https://dspace-erf.nlr.nl/server/api/core/bitstreams/783e9f1d-0503-44bd-acea-48b1636888e0/content (дата обращения: 17.06.2025).

4. Lee B. Numerical simulation of rotor-fuselage aerodynamic interaction using an unstructured overset mesh technique / B. Lee, M. Jung, O.-J. Kwon, H.J. Kang // International Journal of Aeronautical and Space Sciences. 2010. Vol. 11, iss. 1. Pp. 1–9. DOI: 10.5139/IJASS.2010.11.1.001

5. Quon E. Unsteady reynolds-averaged navier-stokes-based hybrid methodologies for rotor-fuselage interaction / E. Quon, M. Smith, G. Whitehouse, D. Wachspress // Journal of Aircraft. 2012. Vol. 49, no. 3. Pp. 961–965. DOI: 10.2514/1.C031578

6. Schäferlein U., Keßler M. CFD-simulation of the rotor head influence to the rotor-fuselage interaction [Электронный ресурс] // 40th European Rotorcraft Forum. United Kingdom, Southampton, 2014. 12 p. URL: https://dspace-erf.nlr.nl/server/api/core/bitstreams/0f0f46c2-f81a-47af-9a73-40c3d6589cf8/content (дата обращения: 17.06.2025).

7. Tan J., Wang H. Numerical analysis of helicopter rotor/fuselage unsteady aerodynamic interaction // Acta Aerodynamica Sinica. 2014. Vol. 32, no. 3. Pp. 320–327. DOI: 10.7638/kqdlxxb-2012.0141

8. Nicolosi F. Fuselage aerodynamic drag prediction method by CFD / F. Nicolosi, P. Vecchia, D. Ciliberti, V. Cusati [Электронный ресурс] // 5th CEAS Air & Space Conference. NL, Delft, 7–11 September 2015. URL: https://www.researchgate.net/publication/332407449_Fuselage_aerodynamic_drag_prediction_method_by_CFD (дата обращения: 17.06.2025).

9. Açıkgöz M.B., Aslan A.R. Dynamic mesh analyses of helicopter rotor–fuselage flow interaction in forward flight [Электронный ресурс] // Journal of Aerospace Engineering. 2016. Vol. 29, no. 6. ID: 04016050. DOI: 10.1061/(ASCE)AS.1943-5525.0000641 (дата обращения: 17.06.2025).

10. Dawei L., Ji X., Jun H. The theoretical research for the rotor/fuselage unsteady aerodynamic interaction problem // Journal of Aerospace Technology and Management. 2016. Vol. 8, no. 3. Pp. 281–288. DOI:10.5028/jatm.v8i3.686

11. Passe B. Identification of rotor-fuselage aerodynamic interactions in a compound coaxial helicopter using CFD-CSD Coupling / B. Passe, A. Sridharan, J. Baeder, R. Singh [Электронный ресурс] // American Helicopter Society Specialists Meeting on Aeromechanics Design for Ver-

tical Lift, CA, San Francisco, 20–22 January 2016. URL: https://www.researchgate.net/publication/296467339_Identification_of_Rotor-Fuselage_Aerodynamic_nteractions_in_a_Compound_Coaxial_Helicopter_using_CFD-CSD_Coupling (дата обращения: 17.06.2025).

12. Batrakov A. Simulation of tail boom vibrations using main rotor-fuselage computational fluid dynamics (CFD) / A. Batrakov, A. Kusyumov, S. Kusyumov, S. Mikhailov, G. Barakos [Электронный ресурс] // Applied Sciences. 2017. Vol. 7, iss. 9. ID: 918. DOI: 10.3390/app7090918 (дата обращения: 17.06.2025).

13. Xu H. A simple and conservative unstructured sliding-mesh approach for rotor-fuselage aerodynamic interaction simulation / H. Xu, S.-L. Xing, Z.-Y. Ye, M.-S. Ma // Proceedings of the Institution of Mechanical Engineers, Part G: Journal of Aerospace Engineering. 2016. Vol. 231, iss. 1. Pp. 163–179. DOI: 10.1177/0954410016664919

14. Aiman W.A. Numerical modelling of helicopter fuselage aerodynamics in forward flight using computational fluid dynamics / W.A. Aiman, N.A.R.N. Mohd, S. Mat, N.B. Dahalan [Электронный ресурс] // 3rd South East Asia Workshop on Aerospace Engineering. Thailand, Bangkok, 6-8 September 2018. URL: https://www.researchgate.net/publication/332038050_NUMERICAL_MODELLING_OF_HELICOPTER_FUSELAGE_AERODYNAMICS_IN_FORWARD_FLIGHT_USING_COMPUTATIONAL_FLUID_DYNAMICS (дата обращения: 17.06.2025).

15. Lorber P., Min B.-Y., Zhao J. (2019). Comparison of rotor - fuselage flow fields and unsteady tail interactions between two CFD codes and experiment [Электронный ресурс] // 75th Annual Forum of the American Helicopter Society. USA, Philadelphia, Pennsylvania, 13–16 May. DOI: 10.4050/F-0075-2019-14500 (дата обращения: 17.06.2025).

16. Kim J., Ko J., Lee S. Aeroacoustic analysis of coaxial rotor with rotor-fuselage interaction [Электронный ресурс] // 48th International Congress and Exhibition on Noise Control Engineering. Spain, Madrid, 16-19 June 2019. 8 p. URL: https://www.sea-acustica.es/INTERNOISE_2019/Fchrs/Proceedings/1812.pdf (дата обращения: 17.06.2025).

17. Zhu Y. Numerical study of the aerodynamic interference of rotors imposed on fuselage for a quadcopter / Y. Zhu, D. Lin, L. Mo, P. Lv, J. Ye [Электронный ресурс] // IEEE Access. 2021. Vol. 9. Pp. 150021–150036. DOI: 10.1109/ACCESS.2021.3124507 (дата обращения: 17.06.2025).

18. Wang C. Main rotor wake interference effects on tail rotor thrust in crosswind / C. Wang, M. Huang, S. Ma, H. Wang, M. Tang [Электронный ресурс] // International Journal of Aerospace Engineering. 2021. Vol. 2021. ID: 9994115. 13 p. DOI: 10.1155/2021/9994115 (дата обращения: 17.06.2025).

19. Аникин В.А. Расчет обтекания корпуса вертолета с помощью уравнений Рейнольдса / В.А. Аникин, А.В. Воеводин, Д.С. Коломенский, Г.Г. Судаков // Полет. Общероссийский научно-технический журнал. 2005. № 11. С. 43–48.

20. Игнаткин Ю.М., Константинов С.Г. Исследование аэродинамических характеристик планера вертолетов методом CFD // Полет. Общероссийский научно-технический журнал. 2017. № 9-10. С. 34–41.

21. Konstantinov S.G. Comparative study of coaxial main rotor aerodynamics in the hover with the usage of two methods of computational fluid dynamics / S.G. Konstantinov, Yu.M. Ignatkin, P.V. Makeev, S.O. Nikitin [Электронный ресурс] // Journal of Aerospace Technology and Management. 2021. Vol. 13. 14 p. DOI: 10.1590/jatm.v13.1210 (дата обращения: 17.06.2025).

22. Ignatkin Yu. Modelling the helicopter rotor aerodynamics at forward flight with free wake model and URANS method / Yu. Ignatkin, P. Makeev, S. Konstantinov, A. Shomov // Aviation. 2020. Vol. 24, no. 4. Pp. 149–156. DOI: 10.3846/aviation. 2020.12714

23. Крицкий Б.С. Пульсации тяги соосного несущего винта, обусловленные взаимным расположением лопастей / Б.С. Крицкий, Р.М. Миргазов, В.А. Аникин, О.В. Герасимов // Научный вестник МГТУ ГА. 2020. Т. 23, № 4. С. 96–104. DOI: 10.26467/2079-0619-2020-23-4-96-104

24. Kim H., Brown R. A comparison of coaxial and conventional rotor performance // Journal of the American Helicopter Society. 2010. Vol. 55, no. 1. Pp. 12004. DOI: 10.4050/JAHS.55.012004

Information about the authors

Sergey G. Konstantinov, Candidate of Technical Sciences, Associate Professor, Associate Professor, the Design and Certification of Aviation Equipment Chair, Moscow Aviation Institute (National Research University), slk.konstantinov@gmail.com.

Pavel V. Makeev, Doctor of Technical Sciences, Associate Professor, Associate Professor, the Design and Certification of Aviation Equipment Chair, Moscow Aviation Institute (National Research University), makeevpv@mai.ru.

Alexander I. Shomov, Candidate of Technical Sciences, Associate Professor, Associate Professor, the Design and Certification of Aviation Equipment Chair, Moscow Aviation Institute (National Research University), shomov_aleksandr@mail.ru.

Сведения об авторах

Константинов Сергей Геннадьевич, кандидат технических наук, доцент кафедры проектирования вертолетов Московского авиационного института, slk.konstantinov@gmail.com.

Макеев Павел Вячеславович, доктор технических наук, доцент, профессор кафедры проектирования вертолетов Московского авиационного института, makeevpv@mai.ru.

Шомов Александр Иванович, кандидат технических наук, доцент, доцент кафедры проектирования вертолетов Московского авиационного института, shomov_aleksandr@mail.ru.

Поступила в редакцию	24.10.2025	Received	24.10.2025
Одобрена после рецензирования	24.11.2025	Approved after reviewing	24.11.2025
Принята в печать	26.03.2026	Accepted for publication	26.03.2026